Volume 143 | Number 7 | 7 April 2018 | Pages 1505–1716

Analyst

rsc.li/analyst

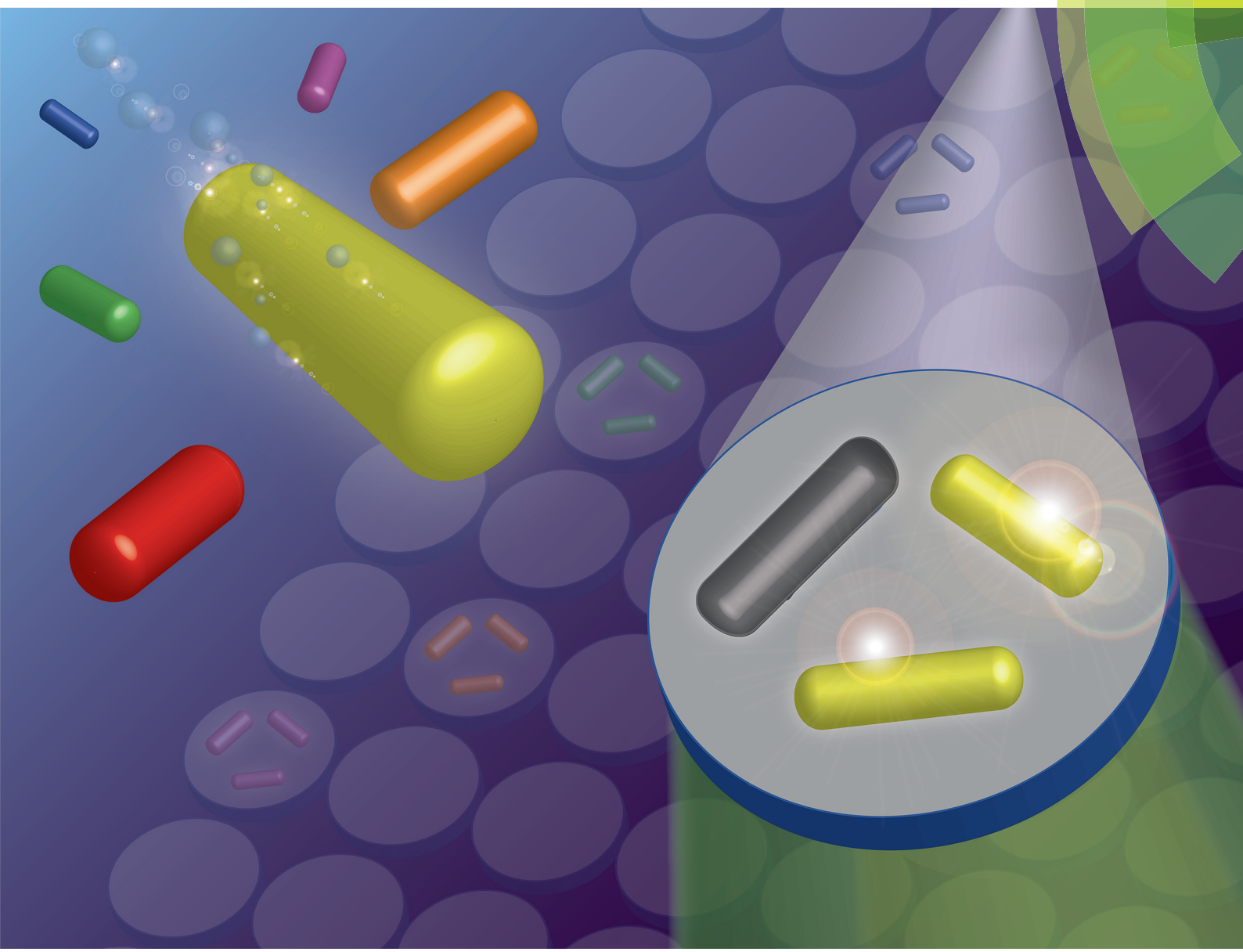

ISSN 0003-2654

ROYAL SOCIETY OF CHEMISTRY

PAPER
Hiroshi Shiigi *et al.*
A rapid and specific bacterial detection method based on cell-imprinted microplates

Analyst

PAPER

View Article Online
View Journal | View Issue

Cite this: *Analyst*, 2018, **143**, 1568

A rapid and specific bacterial detection method based on cell-imprinted microplates†

Xueling Shan,[a] Takuya Yamauchi,[a] Yojiro Yamamoto,[a,b] Hiroshi Shiigi *[a] and Tsutomu Nagaoka[a]

Received 20th December 2017,
Accepted 19th January 2018

DOI: 10.1039/c7an02057k

rsc.li/analyst

Bacterial detection has attracted substantial interest in recent years owing to its importance in biology, medical care, drug discovery, and public health. For such applications, bacterial cell-imprinting technologies are regarded as potential methods, as they can fabricate artificial tailor-made receptors for cellular recognition. In comparison to conventional methods, which generally require a few days for bacterial determination, cell-imprinted polymers can save a substantial amount of time. Here, we report a high-throughput bacterial detection method based on a cell-imprinted 96-well microplate. The fabrication of the bacterial cell-imprinted polypyrrole and nafion complex was accomplished on a gold nanoparticle-coated microplate. The cell-imprinted polymer complex on the microplate can spontaneously rebind and specifically detect target cells with high selectivity in a short time frame (within 30 min). Furthermore, the microplates could discriminate particular target *Escherichia coli* O157:H7 cells from bacterial mixtures. This simple method may be used for a variety of applications such as clinical testing, food safety, and continuous environmental monitoring.

Introduction

Bacteria are an indispensable component of the world's ecosystems and are essential for the survival of mankind. Most bacteria are helpful and/or have no effect on human health, whereas a few cause severe disease.[1] These pathogenic bacteria, including *Anthrax bacillus*, *Yersinia pestis*, *Helicobacter pylori*, and *Escherichia coli*, have attracted substantial interest because they are susceptible to causing infection and lead to high mortality rates.[2] Therefore, the rapid detection and identification of pathogenic bacteria in foods, clinical samples, and in the environment represents an effective method for the prevention of epidemic outbreaks, and allows the implementation of timely treatments and response measures.[3] However, the conventional colony counting method, which allows for accurate bacterial identification, is suboptimal in ensuring a rapid response to an epidemic, as it requires a multistep process with long-term culturing time of over 24 h. Therefore, nonculture-based methods such as antigen–antibody assays, enzyme-linked immune-sorbent assays (ELISA), fluorescence activated cell sorting, and cell-imprinted polymers (CIPs) have been proposed.[4] Among these methods, CIPs, which are based on the molecular imprinting technique, are useful for the fabrication of artificial receptors.[5] This technique allows for the rapid formation of cavities that bind specifically to the various desired targets. In contrast, antibodies, which are naturally produced as conventional receptors by the immune system, require several months to produce.

Microplate methods that enable high-throughput screening are commonly used in ELISA, and represent the basis of most modern medical diagnostic tests in humans and animals.[6] Recently, it was discovered that the combination of molecular imprinting and microplates presented unforeseen advantages. For example, Piletsky *et al.* have effectively grafted epinephrine imprinted poly-(3-aminophenylboronic acid), which acts as an artificial adrenergic receptor, onto microplate wells for the determination of β-agonists.[7] The formation of the artificial receptor on the polymer increased the affinity toward epinephrine and displayed high stability and good reproducibility when compared to conventional antibodies. Bi and Liu introduced a polymer-coated microplate for imprinting α-fetoprotein, thus establishing a molecular imprinted polymer (MIP)-based ELISA method that exhibited excellent specificity, high binding strength, fast equilibrium kinetics, and reusability.[8] In addition, several studies have revealed that the MIP method represents an attractive alternative to conventional antibodies or receptors.[9]

[a]*Department of Applied Chemistry, Osaka Prefecture University, 1-2 Gakuen, Naka, Sakai, Osaka 599-8570, Japan. E-mail: shii@chem.osakafu-u.ac.jp; Tel: +81 72 254 9875*

[b]*GreenChem. Inc., 19-19 Tsuruta, Nishi, Sakai, Osaka 593-8323, Japan*

†Electronic supplementary information (ESI) available: Additional figures. See DOI: 10.1039/c7an02057k

Previously, we reported that cell-imprinted polypyrrole (PPy) and nafion polymer complex-coated microspheres specifically and spontaneously recognised target cells and were useful for recovery and quantification.[10] However, it was difficult to evaluate the role of the polymer complex on the microsphere surface owing to the 3-dimensional micrometer-sized substrate characteristic. Moreover, quantification based on the light-scattering of single microsphere was time-consuming, requiring 5 hours at least. Based on these considerations, we proposed that the generation of bacterial CIPs within microplate wells may prove a very effective alternative, owing to the potential rapid signal acquisition, high-throughput detection, and convenient operation process. Herein, we discuss the preparation of CIPs onto microplates for the rapid detection and identification of bacterial cells.

Experimental

Materials and reagents

All chemical reagents were of analytical grade and used as supplied without further purification unless indicated. Pyrrole was obtained from Wako Pure Chemical Industries (Japan). Nafion®117 and SYTO9® were purchased from Sigma-Aldrich and Thermo-Fisher Scientific, respectively. Nutrient broth (NB) was obtained from Eiken Chemicals (E-MC35, Japan). Ultrapure water (resistance >18 MΩ) was used throughout this study.

For safety reasons, the experiments were conducted using genetically modified verotoxin-nonproducing *E. coli* PV856 (O157:H7), *E. coli* PV03-017 (O26:HNM), and *E. coli* PV01-198 (O26:H11) strains. *E. coli* K-12 (O Rough), *Acinetobacter calcoaceticus* (no. 13006), and *Serratia marcescens* (no. 3736) were acquired from the Biological Resource Center, National Institute of Technology and Evaluation (NBRC, NITE, Japan).

Apparatus

Samples were imaged using a TM3030 (Hitachi, Japan) scanning electron microscope, operating at an accelerating voltage of 5 kV, and using multimode atomic force microscopy (NanscopeIIIa, Veeco). Amino and carboxy group-functionalised polystyrene 96-well microplates (MS-8696F and MS-8796F, Sumitomo Bakelite, Japan) were used for all experiments. Fluorescence intensities were collected *via* an ARVO X3 multimode plate reader (PerkinElmer). Fluorescence and bright-field images were obtained using an EVOS FL Auto microscope (Life Technologies).

Bacterial culturing

All experiments involving bacterial cultures were executed in a biosafety level 2 laboratory, designed and managed in accordance with safety regulations. The *E. coli* O157:H7 strain was cultured at 303 K for 18 h in NB agar broth. Similarly, colonies were suspended in 30 mL NB liquid growth medium and cultured at 303 K for 18 h. After centrifugation at 7000*g* for 15 min, the supernatant was removed. The pellet was resuspended into fresh phosphate buffer by shaking for 1 min. The suspension was centrifuged using the same conditions described above. These procedures were repeated three times.

Preparation of cell-imprinted microplates

An aminoethanethiol-coated gold nanoparticle (Au NP) dispersion (0.028 wt%, 0.40 mL, pH 2.8) was added into a well on the microplate and incubated for 12 h at 298 K. Following the removal of the dispersion and drying, 0.20 mL of 25 vol% of aqueous ethanol containing 0.40 vol% nafion was added and the microplate was shaken for 3 h. Next, pyrrole monomers (108 mM, 25 μL) and the *E. coli* O157:H7 suspension (50 μL, 3.8×10^9 cells per mL) were added into the well and shaken for 30 min. Subsequently, polymerisation was induced through the addition of a 120 mM ammonium persulfate solution (25 μL) as an oxidant for 12 h at 298 K. Next, overoxidation was achieved through the addition of 0.40 mL of a 0.10 M NaOH solution into the well.[11] After a 3 h incubation, the well was washed with a large amount of ultrapure water until a neutral pH was detected.

Non-imprinted polymer (NIP)-coated microplates were prepared by following the steps described above without adding the template cells.

Binding performance

Following the centrifugation of the *E. coli* O157:H7 suspension at 7000*g* for 15 min, the pellet was resuspended into 1.0 mL of phosphate buffer (pH 6.9). Next, the SYTO9 stain (5.0 μM, 1.0 mL) was added into the suspension for cell labelling. After incubation for 30 min, the suspension was centrifuged at 12 000*g* for 30 min and the excess dye was removed by discarding the supernatant. The pellet was resuspended in phosphate buffer and the sample suspensions were prepared. A suspension of 0.10 mL of the *E. coli* O157:H7 cells labelled with SYTO9 ($40 - 1.9 \times 10^7$ cells per mL) was added into the CIP-based wells. After incubation, the suspensions were removed and washed with phosphate buffer to remove nonspecifically bound cells. For each well, the fluorescence intensity at 535 nm was measured immediately and the number of cells was counted by observation under fluorescence microscopy.

Results and discussion

Characterisation of the cell-imprinted polymer

Firstly, we attempted to deposit the cell-imprinted PPy onto a carboxy group-functionalised microplate. Theoretically, PPy which has a positively-charged backbone, should be favourably formed on a negatively charged surface. However, the polymerisation proceeded only in the bulk solution, and no PPy film was formed on the bottom and wall of the well (Fig. S1A†). In the same manner, it was impossible to form the PPy film on the inner surfaces of either amino group-functionalised or unfunctionalised polystyrene microplates.

To modify the well surface, we used Au NPs, which can be modified with various molecules. Fig. 1A shows a photograph

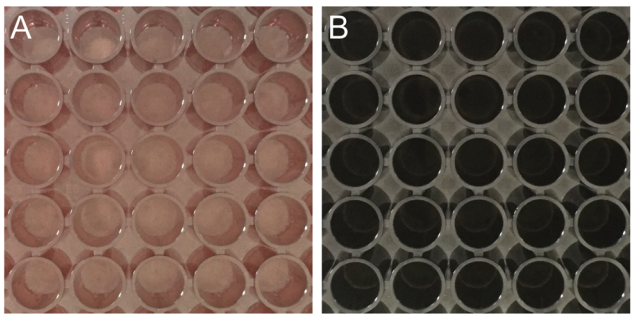

Fig. 1 Photographs of (A) the Au NP-coated microplate and (B) the PPy formed on the microplate.

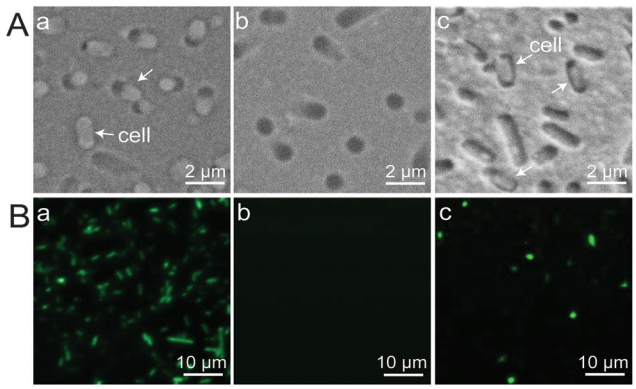

Fig. 2 (A) SEM and (B) fluorescence images of the polymer complex formed on the bottom of the well (a) before and (b) after overoxidation, and (c) after incubation with the *E. coli* O157:H7 suspension (1.9×10^6 cells per mL).

of the Au NP-coated microplate. The Au NPs, which have a positive zeta potential (+36 mV),[12] interacted electrostatically with the carboxy group-functionalised surface of the wells. A uniform reddish coating of Au NPs, as revealed by localised surface plasmon resonance (LSPR), was observed in all wells. This indicated that the Au NPs bound dispersedly, rather than as aggregates.

The thiol groups of aminoethanethiol molecules adsorb onto the Au NP surface through chemisorption and form a monolayer, whereas the amino group electrostatically interacts with the polyelectrolyte nafion.[13] During the nafion-modification process, no apparent change in the LSPR of Au NPs was observed. The formation of the PPy film on the inside wall of the well is shown in Fig. 1B; the polymerisation proceeded both in the bulk solution and on the wall. This indicated that the pyrrole monomers were attracted, through electrostatic interactions and hydrogen bonding, to the laminated inner wall. Initiated by the presence of nafion, the polymerisation proceeded preferentially on the surface of the inside wall of the well, and the thickness of the PPy that resulted was in the appropriate range for cell imprinting.[10]

Scanning electron microscopy (SEM) and fluorescence imaging clearly demonstrated that the *E. coli* cells were entrapped in the polymer complex layer, as shown in Fig. 2Aa. Numerous fluorescent spots, indicating the SYTO9-labeled *E. coli* cells, were observed (Fig. 2Ba). We have previously reported the complete removal of bacterial cells by overoxidising PPy in an aqueous 0.10 M NaOH solution.[14] Similarly, in the current study, no cells remained in the polymer layer following overoxidation. This reaction efficiently removed the bacterial cells from the polymer layer and thereby exposed the bacilli-like cavities, complementary to *E. coli* (Fig. 2Ab). As a matter of course, the bacteria died in the strong alkaline medium (pH 13). As the lipopolysaccharides, hydrophobic lipid moieties, and membrane proteins in the outer membrane were damaged and denatured, the outer membranes of the cells were broken and disassembled. Thus, the cells were completely removed from the polymer layer following the overoxidation process, and therefore no fluorescence signals were observed (Fig. 2Bb). Furthermore, following observation of the polymer-coated microplate using bright-field microscopy (Fig. S2†), a marked difference was detected between before and after overoxidation. The incident light was scattered by the bacterial cells, which consist of 70% water, owing to the difference in the refractive index between water and the matrix polymer complex. In contrast, the incident light passed directly through the bottom of the cavities, without scattering. Therefore, we found that the white spots had shrunk following overoxidation.

Notably, no cracking or peeling of the polymer layer was observed after overoxidation, suggesting that nafion is sufficiently adhesive and forms a structurally robust intertwined network with PPy. To investigate the ability of target cells to rebind the CIP-coated microplate, 100 μL of the *E. coli* suspension (1.9×10^6 cells per mL) was added to the CIP-coated microplate. After 1-hour incubation, the suspension was removed and the well was washed with 0.10 mL phosphate buffer. As observed in SEM and fluorescence images, cells were spontaneously captured by the preexisting cavities (Fig. 2Ac and Bc).

Fig. 3 shows the surface of the polymer complex, examined by atomic force microscopy, before and after overoxidation. We determined the area occupied by a single bacterial cell on the surface of the polymer by estimating the length (2.2 μm), width (0.95 μm), and height (0.49 μm) of the cells, which resulted in a surface area of 3.8 μm^2, on average. Following the overoxidation of PPy, the size of the cavity was estimated as: 1.8 μm in length, 0.87 μm in width, and 0.12 μm in depth. The surface area of the created cavity was calculated at 0.81 μm^2, on average. We concluded that approximately 18% of a cell was buried in the polymer layer, as the surface area of one cell was estimated at 4.4 μm^2 (at a length of approximately 2.0 μm and a diameter of about 0.65 μm). The surface area of the cavity increased with the thickness of the polymer layer. The binding affinity between the cavity and the cell might thus potentially be enhanced by increasing the surface area of the cavity.

Optimisation of the thickness of the cell-imprinted polymer

Hydrogen bonding, chemisorption, and electrostatic interactions in an organic–inorganic hybrid allow for the formation

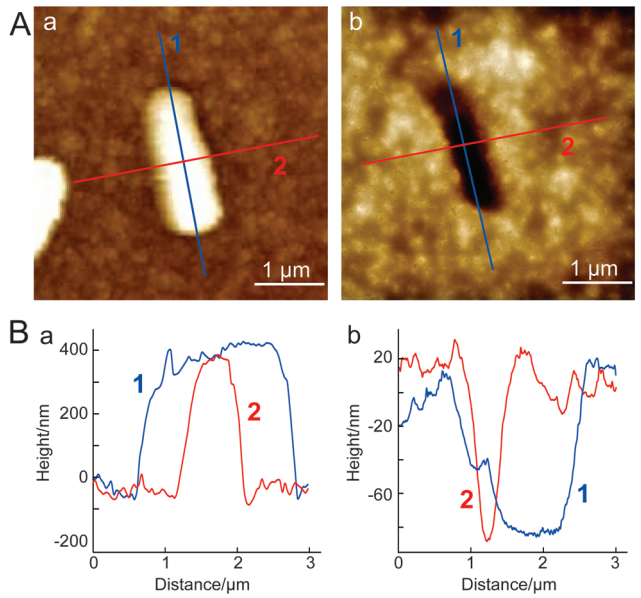

Fig. 3 (A) Atomic force microscopy images and (B) cross-sectional profiles, corresponding to the polymer complex formed on the bottom of the well (a) before and (b) after overoxidation.

of a robust matrix for cell imprinting, and of a scaffold for cell recognition, through the self-arrangement of functional groups. To attain cell recognition with high accuracy, it was therefore necessary to optimise the thickness of the polymer complex. The formation of a shape-complementary cavity of an appropriate thickness on the layer enhances the binding affinity for target cells. To determine the optimal conditions for the preparation of cell-complementary cavities on the microplate, the concentration of the pyrrole monomer was investigated (Fig. 4). Shallow cavities were observed on the polymer complex when the concentration of pyrrole was less than 27 mM. Conversely, some cells were fully covered by PPy and buried deeply in the layer at a higher concentration of the monomer (over 270 mM). In this case, many cells were retained in the polymer layer following overoxidation. Thus, we hypothesised that the size of the cavity that was formed on the polymer complex when prepared at a pyrrole concentration of 108 mM and a nafion concentration of 0.40 vol% (Fig. S1B†), was close to the dimensions of the original cells (refer to Fig. 3). Therefore, the polymer complex layer formed under these conditions was used in the following experiments.

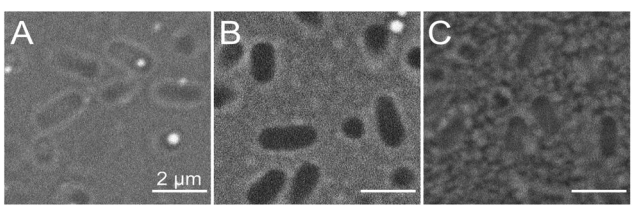

Fig. 4 SEM images of the *E. coli* O157:H7 cell-imprinted polymer layer formed on the bottom of well, at a pyrrole concentration of (A) 27 mM, (B) 108 mM, and (C) 270 mM.

Characterisation of binding performance

The binding affinity of the CIPs on the microplate for target cells was investigated by using *E. coli* O157:H7 cells, labelled with the SYTO9 membrane-permeant nucleic acid stain.[15] Following incubation in the presence of the cells, the bacterial suspension was removed and the fluorescence intensity on the microplate was recorded using a plate reader. The fluorescence drastically increased within 15 min and became constant after 30 min (Fig. 5A), which indicated that the CIPs captured cells spontaneously. This spontaneous binding allows for a rapid response and minimises the decrease in the fluorescence of the dye. To determine the relationship between fluorescence and number of bacterial cells, we employed a 1-hour incubation using various concentrations of *E. coli* cultures. Following the removal of the suspensions, the microplate was washed with 0.10 mL of phosphate buffer.

Next, the fluorescence intensities on the microplate were determined, as shown in Fig. 5B. The fluorescence intensity of the CIP-coated microplate strongly depended on the number of *E. coli* cells, and increased proportionally with the increase

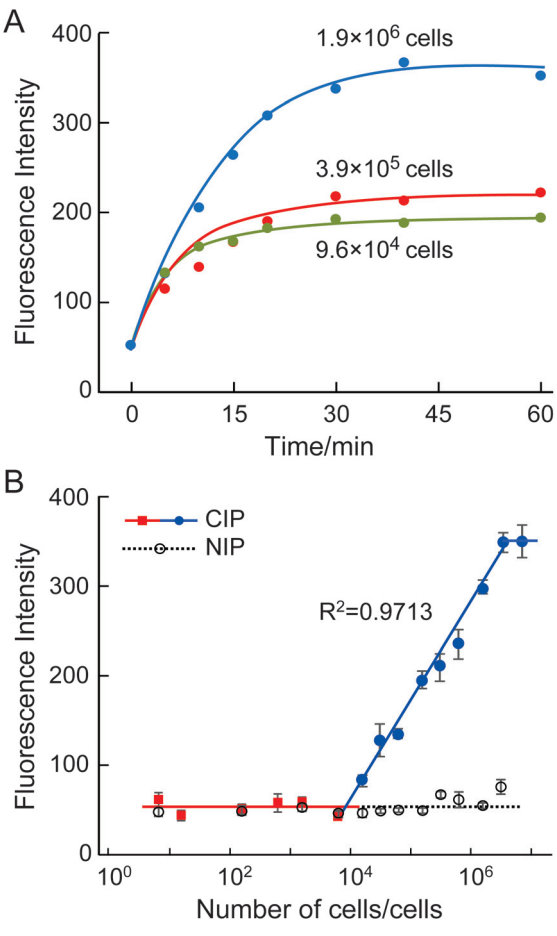

Fig. 5 (A) Time course of the fluorescence intensity on the CIP-coated microplate. The number of the *E. coli* O157:H7 cells are indicated in the figure. (B) Dependence of the fluorescence intensity of the CIP- and NIP-coated microplates on the number of *E. coli* cells in the well (n = 3).

in the number of the cells from 3.9×10^3 to 1.9×10^6 cells, with a high correlation coefficient (R^2 = 0.9713). The fluorescence reached a plateau above 1.9×10^6 cells. Conversely, no difference in the fluorescence intensity was observed between 1.9×10^6 cells and 3.9×10^6 cells. This was attributed to saturation of target cell rebinding into the cavity at 1.9×10^6 cells. By SEM observation, we estimated that a total of 4.8×10^6 cavities were formed on each well. This indicates that 40% of the total number of cavities formed on the polymer complex functioned as recognition sites. From the intersection of the intercept and the slope, we could also estimate that the limit of detection was 5.1×10^3 cells. Moreover, we also counted the number of cells on the well using fluorescence microscopy. At the detection limit, the rebound cell number was counted at approximately 2500 cells per well, corresponding to 50% of the total number of cells in the suspension. Therefore, it was found that there was equilibrium between target cells and active cavities. Conversely, there was no fluorescence intensity observed on the NIP-coated microplate. This indicated that non-specific absorption of bacterial cells could be removed easily through the washing step.

Selectivity

High throughput detection requires high selectivity as well as rapidity. Therefore, we tested the *E. coli* O157:H7 cell-imprinted polymer-coated microplate against suspensions containing different types of bacterial cells, such as *E. coli* O26:H11, *E. coli* O Rough, *Serratia marcescens*, and *Acinetobacter calcoaceticus*, at a concentration of 1.9×10^6 cells per mL. After 1-hour incubation, the respective suspension was removed from the CIP-coated well. The fluorescence intensity of the well (I) was measured using a plate reader. The intensity for the target *E. coli* O157:H7 cells (I_0) was approximately 20-fold higher than that for the different types of bacteria, thus highlighting the specificity of the microplate, with an $I/I_0 < 0.06$, as shown in Fig. 6A. The number of cells captured on the CIPs was also counted using fluorescence microscopy (Fig. 6B). It was confirmed that the CIPs formed on the microplate presented a high cell-recognition ability that was based on their specific binding characteristics.

To apply our technique toward high-throughput bacterial detection, we prepared a cell-imprinted microplate using the various types of bacterial cells as a template. After a 1-hour incubation, the intensities obtained for the respective target cells were higher than those for the different types of bacteria (Fig. 6C). The selectivity, which was obtained from the fluorescence intensity for the respective cell suspension divided by that of the template cell, indicated over 10-fold preference for the respective targets than for the different bacterial types.

It has been reported that the specificity of the polymer was not only based on the size and shape of the cells, but also on bacterial surface structures,[16] as it was able to distinguish between different strains of *E. coli* with similar sizes and shapes. In the polymer complex, the functional groups included in nafion (*e.g.*, sulpho and fluoro) and PPy (*e.g.*, amino, imino and carbonyl[11,17]) were arrayed through electrostatic interaction and hydrogen bonds on the inner surface of the cavities.[10] The array was formed when the template was doped in the complex. The template information, including its

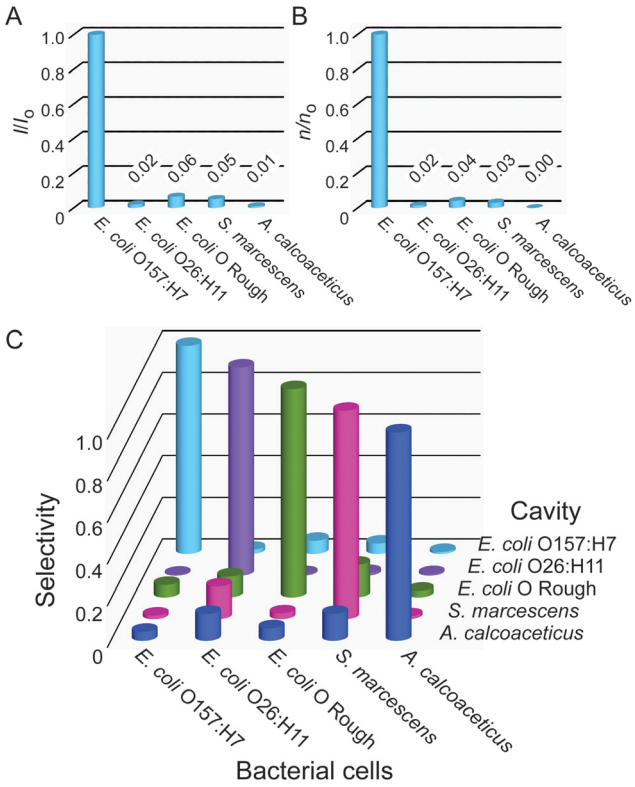

Fig. 6 (A) The uptake ratio (I/I_0), obtained from the fluorescence intensities, where I is the fluorescence intensity for the test strain and I_0 is the fluorescence intensity for the *E. coli* O157:H7 strain (n = 3). (B) The uptake ratio (n/n_0), calculated from the number of cells bound to the microplate, where n indicates a test strain and n_0 indicates the *E. coli* O157:H7 strain (n = 3). (C) Selectivity of various types of cavity (n = 3). The selectivity was calculated from the fluorescence intensity obtained for the respective cell suspension divided by that of the template cell (n = 3).

Table 1 Recovery of the CIP-coated microplate for mixtures of strains (n = 3)[a]

Sample[b]	Bacterial cell	Recovery[c] %
Target	*E. coli* O157:H7	100
Mixture 1	*E. coli* O157:H7	100 ± 11
	E. coli O26:H11	
	E. coli O26:HNM	
	S. marcescens	
	A. calcoaceticus	
Mixture 2	*E. coli* O26:H11	8.2 ± 3.9
	E. coli O26:HNM	
	S. marcescens	
	A. calcoaceticus	

[a] The recovery was calculated as I/I_0 from the fluorescence intensity obtained for mixtures (I) and the *E. coli* O157:H7 (I_0) strain. [b] The concentration of each cell in the suspension was 1.9×10^6 cells per mL. [c] The fluorescence intensity of mixtures at 535 nm was recorded using the plate reader.

size and shape as well as the chemical structures of the surface, could be accurately transcribed as molecular recognition sites on the complex. Therefore, the cavities interacted with the targets at multiple points. Although functional groups were also present outside of the cavity, their array did not correspond to the template.

The selectivity of the CIP-coated microplate was further investigated using an interference assay for mixture samples, which included different types of bacterial cells (Table 1). We found that the recovery of mixture 1 was approximately 100%, indicating that the microplate could discriminate the target strain from other types of strains. Conversely, the recovery of mixture 2 was considerably decreased, as the *E. coli* O157:H7 strain was absent from this mixture.

Conclusions

In summary, we present an effective approach for bacterial recognition using a cell-imprinted polymer complex formed on a 96-well microplate. We observed a rapid (within 30 min), highly-selective identification of bacterial cells. The polymer on the microplate could discriminate the target strain from other strains with high selectivity (approximately 20-fold), which was caused by the accurate imprinting of 18% of the surface structures of a single cell onto the polymeric film. The chemical structure of the polymer complex provided an array of functional groups and allowed for the formation of a shape-complementary cavity. The resulting surface of the polymer could bind target cells spontaneously, with a high accuracy and specificity. This approach may represent an effective alternative to conventional culturing or receptors, and it may also lead to many novel developments in the field of life sciences.

Conflicts of interest

There are no conflicts to declare.

Acknowledgements

This work was supported by the Japan Society for the Promotion of Science through a Grant-in-Aid for Scientific Research (B) (KAKENHI 16H04137) and a Grant-in-Aid for Challenging Exploratory Research (KAKENHI 26620072). X. S. acknowledges the financial support received from the Otsuka Toshimi Scholarship Foundation through a Grant-in-Aid for the scholarship recipient.

Notes and references

1 C. R. Woese, O. Kandler and M. L. Wheelis, *Proc. Natl. Acad. Sci. U. S. A.*, 1990, **87**, 4576; R. N. Glud, F. Wenzhöfer, M. Middelboe, K. Oguri, R. Turnewitsch, D. E. Canfield and H. Kitazato, *Nat. Geosci.*, 2013, **6**, 284; S. Hagedorn and B. Kaphammer, *Annu. Rev. Microbiol.*, 1994, **48**, 773; H. Shiigi, T. Kinoshita, M. Fukuda, D. Q. Le, T. Nishino and T. Nagaoka, *Anal. Chem.*, 2015, **87**, 4042; T. Kinoshita, D. Q. Nguyen, D. Q. Le, K. Ishiki, H. Shiigi and T. Nagaoka, *Anal. Chem.*, 2017, **89**, 4680; P. Sansonetti, *Bacterial Virulence Basic Principles, Models and Global Approaches*, Wiley, Weinheim, 2010.

2 J. E. LeClerc, B. Li, W. L. Payne and T. A. Cebula, *Science*, 1996, **274**, 1208; C. M. Courtney and A. Chatterjee, *ACS Infect. Dis.*, 2015, **1**, 253; World Health Organization, *Global Tuberculosis Report*, WHO, Geneva, 2012.

3 T. Kinoshita, D. Q. Nguyen, D. Q. Le, K. Ishiki, H. Shiigi and T. Nagaoka, *Anal. Chem.*, 2017, **89**, 4680; H. Shiigi, M. Fukuda, T. Tono, K. Takada, T. Okada, D. Q. Le, Y. Hatsuoka, T. Kinoshita, M. Takai, S. Tokonami, H. Nakao, T. Nishino, Y. Yamamoto and T. Nagaoka, *Chem. Commun.*, 2014, **50**, 6252.

4 N. Kobayashi and H. Oyama, *Analyst*, 2011, **136**, 642; A. Ambrosi, F. Airò and A. Merkoçi, *Anal. Chem.*, 2010, **82**, 1151; G. Yang, J. R. Rich, M. Gilbert, W. W. Wakarchuk, Y. Feng and S. G. Withers, *J. Am. Chem. Soc.*, 2010, **132**, 10570; A. Aherne, C. Alexander, M. J. Payne, N. Perez and E. N. Vulfson, *J. Am. Chem. Soc.*, 1996, **118**, 8771; P. Wongkongkatep, K. Manopwisedjaroen, P. Tiposoth, S. Archakunakorn, T. Pongtharangkul, M. Suphantharika, K. Honda, I. Hamachi and J. Wongkongkatep, *Langmuir*, 2012, **28**, 5729.

5 S. Tokonami, Y. Nakadoi, M. Takahashi, M. Ikemizu, T. Kadoma, K. Saimatsu, L. Q. Dung, H. Shiigi and T. Nagaoka, *Anal. Chem.*, 2013, **85**, 4925; K. Ren and R. N. Zare, *ACS Nano*, 2012, **6**, 4314; A. L. Bole and P. Manesiotis, *Adv. Mater.*, 2016, **28**, 5349; R. Schirhagl, E. W. Hall, I. Fuereder and R. N. Zare, *Analyst*, 2012, **137**, 1495.

6 Z. Qu, H. Xu, P. Xu, K. Chen, R. Mu, J. Fu and H. Gu, *Anal. Chem.*, 2014, **86**, 9367; R. C. Murdock, L. Shen, D. K. Griffin, N. Kelley-Loughnane and I. Papautsky, *Anal. Chem.*, 2013, **85**, 11634.

7 S. A. Piletsky, E. V. Piletska, B. Chen, K. Karim, D. Weston, G. Barrett, P. Lowe and A. P. Turner, *Anal. Chem.*, 2000, **72**, 4381.

8 X. Bi and Z. Liu, *Anal. Chem.*, 2014, **86**, 959.

9 S. A. Piletsky, E. V. Piletska, A. Bossi, K. Karim, P. Lowe and A. P. Turner, *Biosens. Bioelectron.*, 2001, **16**, 701; X. Bi and Z. Liu, *Anal. Chem.*, 2014, **86**, 12382.

10 X. Shan, T. Yamauchi, Y. Yamamoto, S. Niyomdecha, K. Ishiki, D. Q. Le, H. Shiigi and T. Nagaoka, *Chem. Commun.*, 2017, **53**, 3890.

11 H. Okuno, T. Kitano, H. Yakabe, M. Kishimoto, B. Deore, H. Shiigi and T. Nagaoka, *Anal. Chem.*, 2002, **74**, 4184; H. Shiigi, D. Kijima, Y. Ikenaga, K. Hori, S. Fukazawa and T. Nagaoka, *J. Electrochem. Soc.*, 2005, **152**, H129.

12 T. Niidome, K. Nakashima, H. Takahashi and Y. Niidome, *Chem. Commun.*, 2004, **17**, 1978.

13 G. He, Z. Li, Y. Li, Z. Li, H. Wu, X. Yang and Z. Jiang, *ACS Appl. Mater. Interfaces*, 2014, **6**, 5362; K. A. Mauritz and R. B. Moore, *Chem. Rev.*, 2004, **104**, 4535.
14 S. Tokonami, H. Shiigi and T. Nagaoka, *Molecularly Imprinted Sensors*, Elsevier B. V., Amsterdam, The Netherlands, 2012, pp. 74–87.
15 Q. Schwartz and M. Bercovici, *Anal. Chem.*, 2014, **86**, 10106.
16 X. Shen, J. S. Bonde, T. Kamra, L. Bülow, J. C. Leo, D. Linke and L. Ye, *Angew. Chem.*, 2014, **126**, 10863.
17 H. Shiigi, M. Kishimoto, H. Yakabe, B. Deore and T. Nagaoka, *Anal. Sci.*, 2002, **18**, 41.